Environmental Pollution 275 (2021) 116613

Contents lists available at ScienceDirect

Environmental Pollution

journal homepage: www.elsevier.com/locate/envpol

Dual-template magnetic molecularly imprinted polymer-based sorbent for simultaneous and selective detection of phenolic endocrine disrupting compounds in foodstuffs[☆]

Shikha Bhogal [a], Irshad Mohiuddin [a], Kuldeep Kaur [b], Jechan Lee [c, d], Richard J.C. Brown [e], Ashok Kumar Malik [a], Ki-Hyun Kim [f, *]

[a] *Department of Chemistry, Punjabi University, Patiala, 147002, Punjab, India*
[b] *Department of Chemistry, Mata Gujri College, Fatehgarh Sahib, 140407, India*
[c] *Department of Environmental and Safety Engineering, Ajou University, Suwon, 16499, Republic of Korea*
[d] *Department of Energy Systems Research, Ajou University, Suwon, 16499, Republic of Korea*
[e] *Environment Department, National Physical Laboratory, Teddington, TW11 0LW, United Kingdom*
[f] *Department of Civil and Environmental Engineering, Hanyang University, Seoul, 04763, Republic of Korea*

ARTICLE INFO

Article history:
Received 10 November 2020
Received in revised form
23 January 2021
Accepted 25 January 2021
Available online 5 February 2021

Keywords:
Alkylphenols
Food
Magnetic dual-template molecularly imprinted polymer
HPLC-PDA

ABSTRACT

In this research, an efficient (94.9–99.4%) and fast (5 min) method has been developed and validated for simultaneous identification and quantification of phenolic endocrine disrupting compounds with an emphasis on bisphenol A (BPA) and 4-cumylphenol (4-CP) in food stuffs using a dual-template magnetic, molecularly-imprinted polymer (dt-MMIP). The dt-MMIP was synthesized by a sol-gel method using $Fe_3O_4@SiO_2$ (as the core) and BPA and 4-CP (as templates). The dt-MMIP was coupled with magnetic solid phase extraction to simultaneously detect BPA and 4-CP in food samples. BPA was measured from bottled water and fruit juice samples samples at 0.36 and 0.24 ng mL^{-1}, respectively, while 4-CP in those samples was 0.33 and 0.16 ng mL^{-1}, respectively. Their detection limits were estimated as 0.04 and 0.05 ng mL^{-1}, respectively. The developed dt-MMIP method was highly reproducible, while maintaining a good cyclability up to 20 cycles.

1. Introduction

Endocrine-disrupting compounds (EDCs) are a category of synthetic and naturally occurring chemicals that can mimic hormones or block their activity in humans and animals (Liu et al., 2011). Among the extensive list of such compounds, phenolic EDCs have drawn considerable attention due to their extensive use in food packaging materials (Berardi et al., 2019). Bisphenol A (BPA), as an example, is used preferably in the production of polycarbonate plastics and epoxy resins commonly used as internal linings in food and drink cans and plastic bottles (Almeida et al., 2018). Likewise, 4-cumylphenol (4-CP) has been used as a raw material for surfactants, fungicides, and preservatives (Chiha et al., 2011). Alkyl phenols (APs) are easily transferred from bottles or packaging materials to edible products, as their presence has been identified in beverages and food products (Kubiak and Biesaga, 2019; Zuo and Zhu, 2014). The use of APs in consumer products is forbidden by law in many European countries, although some APs (including BPA and 4-CP) are still utilized in consumer products in many Asian countries (Wang et al., 2012). The possible leaching of APs into foodstuffs can pose a threat to consumers' health. Therefore, sensitive analytical methods are needed for accurate quantification of these harmful substances.

Molecularly imprinted polymers (MIPs) have been used extensively in chromatography (Mohiuddin et al., 2020), chemical sensing (Lahcen and Amine, 2019), and catalysis (Muratsugu et al., 2020). Their potential utility of solid phase extraction (SPE) in combination with chromatographic analysis has been recognized because of their selectivity toward target analytes and the reusability of the sorbent. This technique enables extraction, clean up, and concentration of analytes prior to quantification (Grover et al., 2019). The use of MIP as an SPE sorbent confers high selectivity toward target analytes in samples with complex matrices (e.g.,

---

[☆] This paper has been recommended for acceptance by Da Chen.
[*] Corresponding author.
E-mail address: kkim61@hanyang.ac.kr (K.-H. Kim).

https://doi.org/10.1016/j.envpol.2021.116613
0269-7491/

foodstuffs) (Arabi et al., 2017). The traditional MIP-based SPE (MIP-SPE) method (where the MIP is packed inside empty SPE cartridges) has many limitations: (1) the need of extra device like control valves to maintain a certain flow rate of sample solution during the analytical process (Hu et al., 2014), (2) possible contamination of the SPE column (due to the presence of impurities), and (3) the occurrence of secondary pollution by plastic column made of polyethylene or polypropylene (e.g., elevation of background levels) (Peng et al., 2010).

Magnetic molecularly imprinted polymer (MMIP)-based SPEs (MMIP-SPE) have received considerable attention as an alternative for MIP-SPE (Ansari, 2017). The MMIP-SPE does not require extra equipment even with large amounts of samples (e.g., up to 1000 mL) and can be used to analyze samples both in solutions and in suspensions (Han et al., 2014). In addition, MMIP-SPE has fast kinetics, easy experimental handling, and may allow automation (Yang et al., 2016). However, typical MMIP-SPE methods are able to analyze only one compound at one time. Development of dual-template imprinting can help expand its applicabilities. As the use of dual-template MMIP in the SPE method does not require synthesis of individual MIP for each analyte, it is useful to lower the cost and analysis times.

In this study, a dual-template MMIP (dt-MMIP) has been prepared by a sol-gel method using $Fe_3O_4@SiO_2$ as a solid support, with BPA and 4-CP as imprinted templates. The dt-MMIP was used as an SPE sorbent for the determination of BPA and 4-CP in food samples (e.g., bottled water, fruit juice, milk, honey, and tomato sauce) based on high-performance liquid chromatography (HPLC). The use of dt-MMIP has already been reported for detection of amphenicol antibiotics (Wei et al., 2016), hydroxyl-cinnamic acids (Dil et al., 2020), and acetaminophen plus codeine (Jafari et al., 2018). In this study, the utility of dt-MMIP is reported for the first time as an SPE-based analytical platform for the quantitation of BPA and 4-CP. The method proposed in this study is expected to provide a simple and sensitive technique to monitor a group of phenolic EDCs such as BPA and 4-CP in foodstuffs.

2. Materials and methods

2.1. Chemicals

In addition to the two key target compounds (i.e., BPA and 4-CP) selected in this work, a list of compounds (dioctyl phthalate (DOP), dicyclohexylphthalate (DHP), benzyl butyl phthalate (BBP), anthracene (ANT), phenanthrene (PHE), *p*-amylphenol (*p*-AP), 3-tert-butylphenol (3-t-BP), *p*-octylphenol (*p*-OP), 3-aminopropyltriethoxysilane (APTES), phenyl trimethoxysilane (PTMOS), tetra ethoxysilane (TEOS), ferric chloride ($FeCl_3.6H_2O$), and ferrous ammonium sulfate ($(NH_4)_2Fe(SO_4)_2\cdot 6H_2O$)) were purchased from Sigma-Aldrich (St. Louis, MO, USA). These chemicals were of analytical grade (>97% purity). HPLC-grade methanol (MeOH), acetonitrile (ACN), toluene, and acetone were supplied by Merck (Mumbai, India). Acetic acid (HAc) and isopropanol (iPrOH) (analytical grade) were obtained from Avra Synthesis. Triply distilled water (TDW) was prepared using distillation equipment (SG Works, India), followed by sonication for degassing prior to use.

2.2. Instruments

Fourier transform infrared spectra (FTIR) were acquired on an RXIFT-IR (PerkinElmer, Japan). The surface morphology was observed using a JEOL JSL-6510LV scanning electron microscope equipped with an energy dispersed spectrum unit (SEM-EDS). Thermogravimetric analysis (TGA) of a sample (5 mg) was performed using an STA7300 TGA instrument (Hitachi, Japan) under a N_2 atmosphere at temperatures from 35 to 800 °C at a heating rate of 10 °C min^{-1}. The specific surface area and pore size were measured by Brunauer-Emmett-Teller (BET) surface area analyzer (Microtrac Belsorp Mini-II, Bel, Japan, Inc). The pH was measured using a Delux pH meter 101 (Electronics India). An REMI RM-12C centrifuge (REMI Laboratory Instruments, India) was used.

All chromatographic measurements were performed using an HPLC system (Waters, USA) equipped with a binary solvent pump (1525) and a photo-diode array (PDA) detector (2998). All separations were achieved with a Waters Spherisorb 5 μm ODS2 HPLC column (4.6 × 250 mm) by isocratic elution using a mobile phase of MeOH and water (9:1; v/v) at a flow rate of 1 mL min^{-1}. The injection volume and detection wavelength were set at 20 μL and 278 nm, respectively. The retention times of BPA and 4-CP were 5.5 min and 6.2 min, respectively.

2.3. Sample preparation

Fruit juice, honey, milk, and tomato sauce were purchased from a local market (Patiala, India). Once opened, they were stored at 4 °C and analyzed within 48 h. A milk sample (5 mL) and tomato sauce (5 g) were added separately to an ACN solution (20 mL) and were subjected to ultra-sonication for 10 min and centrifugation at 10,000 rpm for 10 min. A fruit juice sample (10 mL) was directly centrifuged at 10,000 rpm for 10 min. Before extraction, each sample (5 mL) was diluted to a 1:1 ratio with TDW.

For honey samples, a sample (20 g) was heated (<40 °C) and homogenized by stirring at 500 rpm for 5 min. After that, honey (10 g) from the as-processed sample was diluted with TDW (100 mL). The bottled water extract was collected from a used bottle, which was filled with boiling water and held overnight. All the samples were filtered through a Grade 1 Whatman filter paper (pore size: 11 μm) and nylon-6,6 membrane filter (0.2 μm per 47 mm).

2.4. Synthesis of dt-MMIP

2.4.1. Synthesis of Fe_3O_4 particles

The Fe_3O_4 particles were prepared via a co-precipitation method (Culita et al., 2016). $FeCl_3\cdot 6H_2O$ (15 mmol) and $(NH_4)_2Fe(SO_4)_2\cdot 6H_2O$ (10 mmol) were dissolved in TDW (60 mL). An NH_4OH solution was added to the solution and kept at 80 °C for 1 h with constant stirring at 700 rpm to form a black magnetic powder. The Fe_3O_4 particles were separated using a magnet and were washed with TDW. The resulting material was dried at 60 °C for 24 h.

2.4.2. Synthesis of Fe_3O_4 @SiO_2 particles

The Fe_3O_4 particles were modified using TEOS at 25 °C for 10 h: (1) Fe_3O_4 particles (1 g) were added to an ethanol-water mixture (60 mL; ethanol/water = 5:1 (v/v)), (2) the resulting suspension was sonicated for 30 min, and (3) NH_4OH solution (10 mL) and TEOS (4 mL) were added promptly to the sonicated suspension. The $Fe_3O_4@SiO_2$ precipitate was separated using a magnet, followed by washing with TDW. The final product was dried at 60 °C for 24 h.

2.4.3. Synthesis of dt-MMIP

For synthesis of dt-MMIP, BPA (0.04 g) and 4-CP (0.04 g) were dissolved in ethanol (40 mL). Then, APTES (200 μL) and PTMOS (200 μL) were added to the solution with stirring for 2 h to form a template-monomer complex. Next, $Fe_3O_4@SiO_2$ (0.5 g), TEOS (800 μL), and NH_4OH (1 mL) were added to the complex with stirring at 700 rpm for 6 h. The final product was washed with TDW. For removal of the template compounds (i.e., BPA and 4-CP), Soxhlet extraction was performed for 5 h with a mixture of MeOH/HAc (MeOH/HAc = 95:5 (v/v)).

Magnetic non-imprinted polymers (MNIP) were prepared using the same process but in the absence of BPA and 4-CP templates. The prepared polymers were dried and stored in a vacuum desiccator at room temperature prior to use.

2.5. *Magnetic SPE procedure*

Detection of BPA and 4-CP using dt-MMIP-SPE was carried out by the following procedures: (1) an aqueous standard solution containing BPA and 4-CP (10 mL) at a concentration of 1 ng mL^{-1} was loaded into a 30 mL glass vial; (2) the dt-MMIP (10 mg) was loaded into the vial, and the mixture was stirred at 500 rpm for 5 min to extract the analytes. (3) The dt-MMIP was separated from the solution using a magnet, and the supernatant was discarded. (4) Desorption of the analyte was induced by MeOH/HAc (MeOH/HAc = 9:1 (v/v); 0.5 mL × 2) under ultra-sonication for 1 min, and the eluate was collected by magnetic separation. (5) The solution was analyzed by the HPLC-PDA system. The dt-MMIP particles were washed with TDW (4–5 times) and then dried under N_2 gas for regeneration experiments.

Selectivity experiments were performed using *p*-AP, 4-t-BP, and *p*-OP as structural analogues and DOP, DHP, BBP, ANT, and PHE as non-structural analogues. The dt-MMIP was placed in solution (10 mL) containing BPA, 4-CP, *p*-AP, 4-t-BP, *p*-OP, DOP, DHP, BBP, ANT, and PHE (1 ng mL^{-1} each) with stirring at 500 rpm for 5 min. After separation of dt-MMIP using a magnet, the analyte was eluted with a MeOH/HAc mixture (0.5 mL × 2) and analyzed using the HPLC-PDA system.

2.6. *Validation of the analytical method*

The linear range and method detection limit (MDL) of the two target compounds were determined along with intra- and inter-day precision. The results were obtained based on the triplicate analysis of calibration curves in the range from 0.1 to 50 ng mL^{-1} ($R^2 > 0.99$). MDL was determined according to the US EPA (Environmental Protection Agency) approach (O'Neill et al., 2002):

$\mathrm{MDL} = t\,(n-1, 1-\alpha = 0.99)\,S.$

Here, $t\,(n-1, 1-\alpha = 0.99)$ is the Student's t value appropriate for a 99% confidence level and a standard deviation estimate with $n-1$ degrees of freedom, and S is the standard deviation of the replicate analyses. The MDL values were calculated to be 0.04 and 0.05 ng mL^{-1} for BPA and 4-CP, respectively. The RSD of the method was calculated as less than 5% via three replicate analysis at 1 ng mL^{-1}. The intra and inter day precisions were seen to range from 2.28 to 3.92% and 2.53–4.1% respectively.

2.7. *Regeneration test*

To evaluate the real ability to regenerate the dt-MMIP, 10 mg of polymer was added to 10 mL of BPA and 4-CP solution at a concentration of 1 ng mL^{-1} and stirred at 500 rpm for 5 min. The dt-MMIP was separated by applying an external magnet. Then, the recovered polymers were eluted with 1 mL (0.5 mL × 2) of MeOH/HAc (9:1 (v/v)) to ensure complete removal of adsorbed BPA and 4-CP. Finally, the polymers were washed with TDW (at least 4 times) and then dried under N_2 gas. The recovered dt-MMIP was further reused for up to 25 additional adsorption-regeneration cycles to evaluate stability and re-usability.

3. Results and discussion

3.1. *Characterization of the dt-MMIP*

3.1.1. *FTIR analysis*

The FTIR spectra were recorded at each step of the dt-MMIP synthesis, as shown in Figure S1 (Supporting information). The Fe_3O_4, Fe_3O_4@SiO_2, and dt-MMIP showed a characteristic absorption band of Fe–O at 558 cm^{-1}, indicating polymerization on the Fe_3O_4 surface (Lu et al., 2019). After modification of the Fe_3O_4 surface by SiO_2, asymmetric stretching of Si–O–Si was observed at 1082, 949, and 794 cm^{-1} (Figure S1b) (Lu et al., 2019). Characteristic peaks at 1621 and 1432 cm^{-1} were attributed to N–H bending (APTES) and Si–C_6H_5 stretching modes (PTMOS), respectively (Gao et al., 2014a; Gao et al., 2014b). This indicated successful fabrication of the MIP layer on the Fe_3O_4@SiO_2 surface.

3.1.2. *SEM-EDS analysis*

As shown in Fig. 1a and b, the Fe_3O_4 particles had heterogeneous, irregular, and poorly defined morphologies. The SiO_2 layer resulted in spherical Fe_3O_4@SiO_2 (Fig. 1c and d). The SiO_2 layer can alter the surface morphology of Fe_3O_4 to enable post-synthetic modification, allowing a coating of MIP onto the Fe_3O_4 surface through sol-gel reactions (Han et al., 2014). Fig. 1e and f shows the morphologies of dt-MMIP as regular and globular agglomerates, respectively, demonstrating porosity and thereby increasing adsorption performance (de Oliveira et al., 2019).

The EDS spectrum of the Fe_3O_4 particles shows the existence of Fe (28.58%) and O (61.89%) (Figure S2a). In the spectrum of Fe_3O_4@SiO_2, a Si (10.69%) signal was observed with a change in content of each element, which can be attributed to the SiO_2 layer (Figure S2b). For the dt-MMIP, there was an increase in content of Si by 14.13%, reflecting the presence of APTES and PTMOS monomers. This suggests that modification of the Fe_3O_4@SiO_2 surface resulted from the MIP shell (Figure S2c, Supporting Information).

3.1.3. *Thermogravimetric analysis*

The TGA was performed from 35 to 800 °C to estimate thermal stability of Fe_3O_4, Fe_3O_4@SiO_2, and dt-MMIP. The mass loss of Fe_3O_4 was approximately 7.7% at <150 °C (Figure S3a, Supporting Information) because of evaporation of water. There was a mass loss of 2.5% between 450 and 600 °C, due possibly to elimination of hydroxyl groups formed on the particle surface during the synthesis process (Mahmoudi et al., 2008). The Fe_3O_4@SiO_2 showed a total weight loss of 15.3% (Figure S3b). The initial mass loss of 11.8%, observed below 150 °C, reflects evaporation of water. The mass loss of about 3.5% between 250 and 400 °C can be attributed to dehydroxylation of $Si(OH)_4$ on the magnetic core surface.

The total mass loss of dt-MMIP was approximately 19.3% (Figure S3c). A mass loss of 5.3% was observed at <150 °C, attributed to water evaporation. A mass loss of 4.1% between 300 and 450 °C could be because of thermal decomposition of the polymer layer to liberate water. A 9.9% mass loss between 600 and 800 °C may indicate dehydration of the SiO_2 layer coated on the Fe_3O_4 surface. These losses indicate successful coating of the imprinted layer onto the Fe_3O_4@SiO_2 surface.

3.1.4. *BET analysis*

The surface area and pore size of the adsorbents are important parameters for the description of the properties of adsorbents as they can affect the analyte retention abilities (Liu and Chen, 2015). Figure S4 shows the N_2 adsorption-desorption isotherm and BJH pore size distribution of dt-MMIP. Figure S4 suggests that dt-MMIP is mainly mesoporous in nature with a physisorption isotherm of Type IV with H3 loop features according to IUPAC classification (Liu

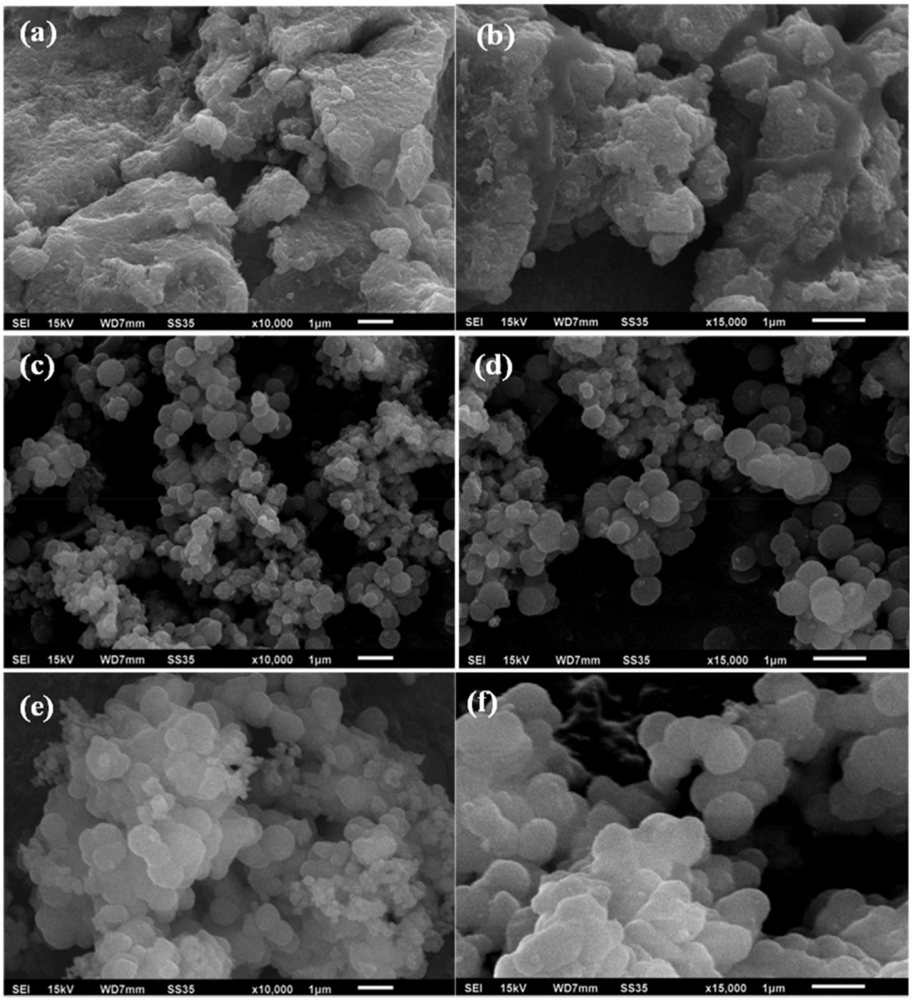

Fig. 1. Scanning electron microscopy images of synthesized materials: Fe_3O_4 (a and b) shows irregular morphology, $Fe_3O_4@SiO_2$ (c and d) shows spherical morphology, and dt-MMIP (e and f) shows spherical agglomerates.

and Chen, 2015). The specific surface area was calculated at 50.68 m^2 g^{-1} by means of BET method. In addition, the mean pore diameter was also calculated as 12.87 nm.

3.2. *Effects of dt-MMIP-SPE parameters*

3.2.1. *Elution solvent*

Selection of an appropriate eluting solvent is essential for maximizing the performance of dt-MMIP-SPE. Elution solvents of toluene, ACN, acetone, iPrOH, MeOH, MeOH/HAc (9:1 (v/v)), MeOH/HAc (8:2 (v/v)), and MeOH/HAc (7:3 (v/v)) were tested. The observed respective recovery percentage and RSD for each of the eluting solvents were: toluene (60.1–62.5%, RSD = 3.9–4.1%), acetone (67.8–69.2%, RSD = 4.0–4.1%), ACN (75.0–76.1%, RSD = 3.1–3.7%), iPrOH (80.5–83.2%, RSD = 2.3–3.6%), and MeOH (94.2–96%, RSD = 2.9–3.5%). Among the tested solvents, MeOH was the most effective eluting solvent, possibly because of its strong H-bonding ability with BPA and 4-CP. When HAc was added to MeOH at three volumetric ratios of 9:1, 8:2, and 7:3, the recovery values (and RSD) were 98.9–99.8% (2.7–3.7%), 91.1–92.5% (2.7–3.4%), and 86.9–89.1% (2.6–3.4%), respectively (Fig. 2a). This was likely because in the presence of HAc, amine group (NH_2) of APTES is protonated (NH_3^+) whereas template molecules (i.e., BPA and 4-CP) remain in their neutral form. Due to the protonation of amine group, the intermolecular H-bonding becomes weakened between APTES and template to cause the desorption of BPA and 4-CP. Further addition of HAc decreased the extraction efficiency (Liu and Chen, 2015). Therefore, MeOH/HAc (9:1 (v/v)) was selected as the elution solvent for the dt-MMIP-SPE method.

3.2.2. *Elution volume and adsorbent loading*

The effect of elution volume on extraction efficiency of BPA and 4-CP was investigated by varying the quantity (0.5, 1, 1.5, and 2 mL) of elution solvent (i.e., MeOH/HAc with a volumetric ratio of 9:1). The best performance was achieved with 1 mL (0.5 mL × 2) of solvent, demonstrating recovery of 98.3–99.7% with an RSD of 2.6–2.7% (Fig. 2b). As an increase in solvent volume to 1.5 or 2 mL (used in portions of 0.5 mL) did not affect recovery, 1 mL (0.5 mL × 2) was chosen for further experiments.

The effect of dt-MMIP loading (2–15 mg) on the extraction process was studied. Extraction recovery increased with an increase in dt-MMIP loading. For example, when dt-MMIP (10 mg) was used, recovery of BPA and 4-CP was maximal (99.80% and 98.66%, respectively). A further increase in dt-MMIP loading to 15 mg did not improve recovery, as shown in Fig. 2c. Thus, 10 mg dt-MMIP was used for further experiments.

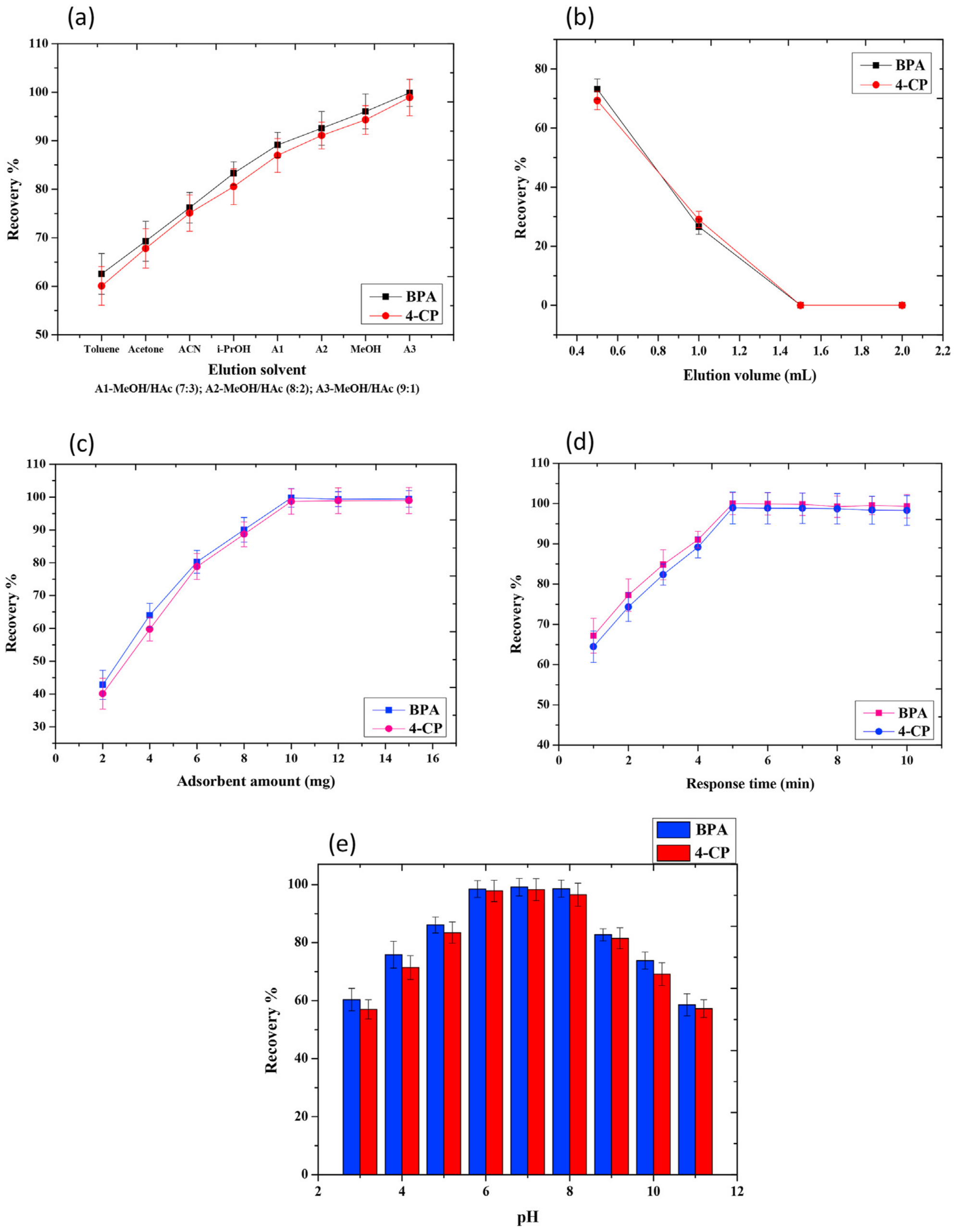

Fig. 2. Factors affecting extraction efficiency of dt-MMIP-SPE against a 1 ng mL^{-1} concentration of BPA and 4-CP: (a) type of elution solvent, (b) elution volume (mL), (c) adsorbent amount (mg), (d) response time (min), and (e) pH effect. Error bars show the relative standard deviations of three replicate extractions.

3.2.3. Extraction time and pH

Extraction time is an important parameter to ensure optimum (or equilibrium) adsorption of analyte onto adsorbent. The effect of extraction time on extraction efficiency of BPA and 4-CP by the dt-MMIP was studied from 1 to 10 min. As shown in Fig. 2d, an increase in recovery value of BPA and 4-CP was observed up to 5 min. After 5 min, the recovery remained almost constant. Therefore, 5 min was sufficient to achieve satisfactory adsorption for recoveries of BPA and 4-CP.

The pH of the sample solution can influence both the dt-MMIP as well as analytes (Lu et al., 2017; Young et al., 2013). The effects of sample pH values in the range of 3–11 were investigated by varying amounts of 0.1 M HCl or 0.1 M NaOH solution. As shown in Fig. 2e, there was no noticeable difference in extraction efficiency at pH 6–8. This behavior can be explained by the net signs of the surface charge of dt-MMIP and template molecules at different pH values. Both BPA and 4-CP mainly exist as neutral molecular forms at pH 6–8. Therefore, there should be no electrostatic repulsion between analytes and the sorbent to support the equivalent extraction recoveries at pH 6–8. A decrease in extraction efficiency was observed when the pH of solution was <6 or >8. With a significant decrease in solution pH, the free hydrogen may become competitive with the –OH groups of the phenolic compounds to form stronger hydrogen bonding with the polymer network of dt-MMIP (Surikumaran et al., 2015). Accordingly, the hydrogen bonding interaction between the analytes (BPA and 4-CP) and the dt-MMIP sorbent is disturbed. Similarly, when the pH of solution was higher than 8, a competition between the –OH groups of the

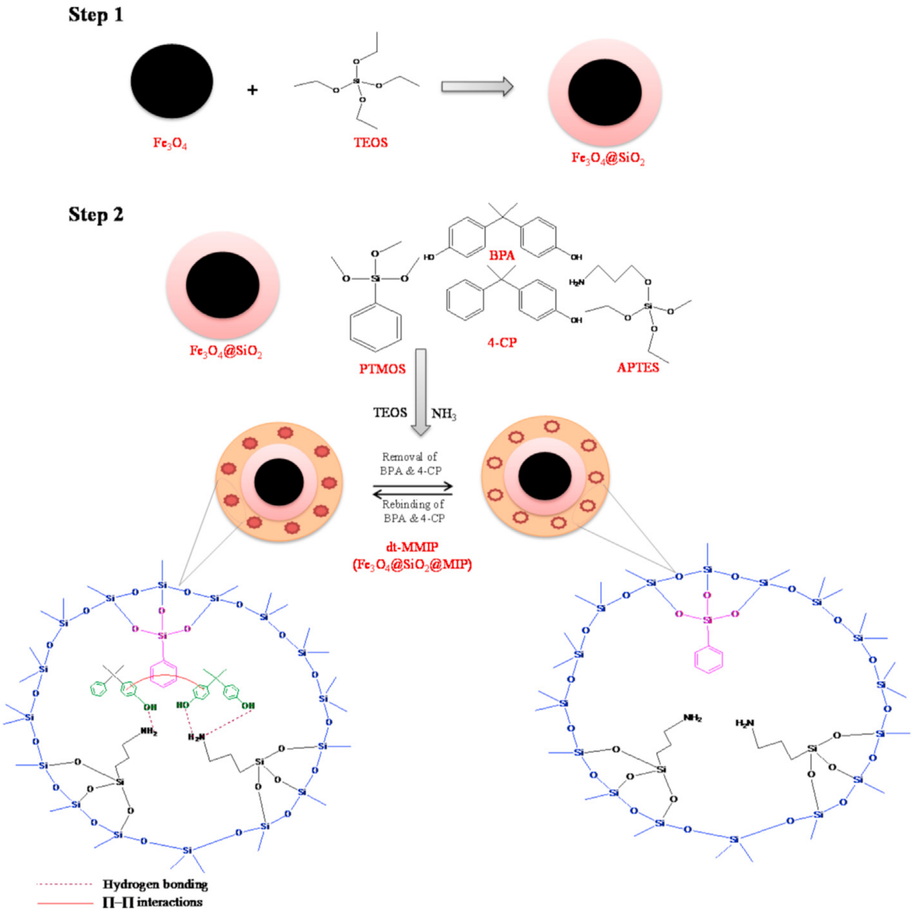

Fig. 3. Schematic of dt-MMIP and its binding mechanism.

alkylphenols could lead to lower recoveries (Surikumaran et al., 2015). Moreover, at high pH values, siloxane bonds can be hydrolyzed by the nucleophillic attack of OH group to deteriorate the chemical bonds in the dt-MMIP. Based on these experimental results, the pH of the sample solution was adjusted to 7 for further experiments after calibration of the electrode with standard buffer solutions at pH 4 and 9.

3.3. Selectivity and specificity studies

The general reaction scheme for dt-MMIP is described in Fig. 3. The surface of the Fe_3O_4 particles was modified with an SiO_2 shell. The modification prevents Fe_3O_4 particles from undergoing oxidation and aggregation, thereby improving the stability and biocompatibility of the material (Lu et al., 2019). The MIP layer on the $Fe_3O_4@SiO_2$ was fabricated via co-polymerization of functional monomers (APTES and PTMOS), a cross linking agent (TEOS), and template molecules (BPA and 4-CP), in the presence of an ammonia solution. Two functional monomers (i.e., APTES and PTMOS) were used to produce imprinting binding sites. APTES can establish hydrogen bonding interactions between its amino groups and hydroxyl groups of the templates. PTMOS can interact with templates by π-π interactions via its phenyl rings (Gao et al., 2014a).

Selectivity tests of the dt-MMIP and MNIP were performed for detecting BPA and 4-CP. The recovery of dt-MMIP toward BPA and 4-CP (98.6–99.8% with RSD = 2.8–3.8%) was higher than that of the MNIP (29.4–31.2% with RSD% = 2.8–3.3), as shown in Figure S5 (Supporting Information). This was because BPA and 4-CP were imprinted on the MMIP layer during synthesis of dt-MMIP. After removal of the templates (i.e., BPA and 4-CP), complementary cavities were established on the dt-MMIP both in size and in shape, leading to effective recognition of BPA and 4-CP. However, the MNIP was non-specific in nature, without complementary cavities for the templates.

The imprinting factor (IF) is commonly used to evaluate the imprinting effect and to measure the strength of interaction between the functional monomer and target molecule (Sullivan et al., 2019). (Note that IF is the ratio of recovery% of dt-MMIP to MNIP.) The higher the IF, the more selective the dt-MMIP is for the target molecule. The IF values obtained for BPA and 4-CP were 3.14 and 3.35, respectively.

To further investigate the selectivity of dt-MMIP toward BPA and 4-CP, experiments were conducted using structural analogues (*p*-AP, 4-t-BP, and *p*-OP) and non-structural analogues (DOP, DHP, BBP, ANT, and PHE). These substances can compete with BPA and 4-CP for binding sites on dt-MMIP as they possess similar functional groups (e.g., carbonyl groups and phenyl ring) capable of interacting with functional monomers (i.e., APTES and PTMOS). The dt-MMIP was placed in solution (10 mL) containing BPA, 4-CP, *p*-AP, 4-t-BP, *p*-OP, DOP, DHP, BBP, ANT, and PHE (1 ng mL^{-1} each) under stirring at 500 rpm for 5 min. The dt-MMIP selectively recognized BPA and 4-CP due to the memory effect of specific binding interactions. The recoveries of BPA and 4-CP (93.9–94.2%) were substantially higher than those of other selected substances (*p*-AP, 4-t-BP, *p*-OP, DOP, DHP, BBP, ANT, and PHE), which showed values < 7%.

3.4. Reproducibility and regeneration of dt-MMIP

In the present research, five batch tests were carried out to assess the reproducibility of synthesized dt-MMIP against BPA and 4-CP. The synthesized dt-MMIP was prepared on different days under identical experimental conditions, as discussed in Section 2.4. Each batch of dt-MMIP was used to extract BPA and 4-CP according to the optimized conditions described in Section 3.2. The recovery of five batches of dt-MMIP for BPA and 4-CP was 98.3–99.9% (Figure S6a, Supporting Information). The reproducibility of five batches of dt-MMIP had an RSD ranging from 2.1 to 3.4%.

Regeneration and reusability of sorbent are important properties to be considered for practical application. In view of cost benefits and environmental protection, the adsorption-desorption cycle was tested over 25 times to evaluate the stability of the dt-MMIP. As shown in Figure S6b (Supporting Information), there was no significant decrease in recovery values over 20 cycles, as recovery values (%) for BPA and 4-CP were maintained in the ranges of 99.9 to 80.0% and 98.8 to 78.0%, respectively. However, a sharper decrease in recovery (from 76.24 to 46.07%) was observed from the 21st to 25th cycles. The decreased adsorption capacity is likely because the imprinting sites in the network of the imprinted polymer were destroyed after continuous rewashing of dt-MMIP.

3.5. Detection of BPA and 4-CP in food samples

The extraction of BPA and 4-CP from real samples (e.g., bottled water, fruit juice, honey, milk, and tomato sauce) was conducted to assess the applicability of the dt-MMIP-SPE method coupled with HPLC-PDA (Table 1). BPA was detected in the bottled water extract, juice, and honey samples at 0.36, 0.24, and 0.11 ng mL^{-1}, respectively. 4-CP was detected in the bottled water extract and fruit juice samples at 0.33 and 0.16 ng mL^{-1}, respectively. As such, BPA and 4-CP were quantified from all samples other than milk and tomato sauce samples.

The concentration levels of BPA and 4-CP measured in foodstuffs were compared with those in previous studies. The observed concentrations of BPA in bottled water were much higher (i.e., 0.36 ng mL^{-1}) in the present study than the previous studies (i.e., 0.07–0.3 ng mL^{-1}) (Gorji et al., 2019; Du et al., 2020). Cesen and coworkers extracted BPA (up to 107 ng/g) in 27 of 36 honey samples using oasis HLB cartridges followed by gas chromatography (Cesen et al., 2016). Their values were much higher than those seen in the present study. The concentration of 4-CP in prawn tissues was reported as 1.96 ng/g (Zuo and Zhu, 2014). However, to the best of our knowledge, no study has reported detection of 4-CP in food stuffs like bottled water extract and juice samples, though they were observed in this study at 0.33 and 0.16 ng mL^{-1}, respectively.

As BPA and 4-CP were below the detection limit (BDL) in the milk and tomato sauce samples, respectively, their quantification was attempted by spiking with different levels of BPA and 4-CP using a standard addition approach (adding quantities of 1, 5, and 10 ng mL^{-1} of BPA and 4-CP). The relative recoveries of spiked BPA and 4-CP in the milk and tomato sauce samples were in the range of 94.9–99.4% with an RSD <5%, indicating good applicability of the method. Fig. 4 shows the HPLC chromatograms of (a) a standard solution of BPA and 4-CP (1 ng mL^{-1}), (b) a standard solution of BPA (1 ng mL^{-1}), (c) a standard solution of 4-CP (1 ng mL^{-1}), (d) bottled water extract, (e) fruit juice sample, and (f) honey sample. The samples were acquired under the optimized conditions described earlier in this paper: mobile phase (MeOH: H_2O, 9:1 (v/v)), flow rate (1 mL min^{-1}), detection wavelength ($\lambda = 278$ nm), injection volume (20 μL), and C-18 column (4.6 × 250 mm).

3.6. Method performance comparison

The performance of the method developed for BPA and 4-CP detection in foodstuffs was compared with those of the previous reports (Table 2). The MDL values for the developed method were in the range of 0.04–0.05 ng mL^{-1} for quantitative analysis of BPA and 4-CP. The concentrations of BPA from bottled water and bottled milk were determined using a self-magnetic nano-composite at a LOD of 0.02–0.38 ng mL^{-1} (Gorji et al., 2019). This detection limit is comparable with that of the present method. Many previous MIP sorbents reported a LOD in the range of 0.3–5.7 ng mL^{-1} for BPA in juice and milk samples. The reported values are lower than those measured by dt-MMIP sorbent (Wu et al., 2014; Yuan et al., 2016; Wu et al., 2017). The Fe_3O_4@MON-NH_2 composites showed the lowest LOD of BPA and 4-CP of 0.015 ng mL^{-1} (Du et al., 2020). However, Fe_3O_4@MON-NH_2 composites exhibited extraction recovery of 80.3–93% for BPA and 4-CP in spiked bottled water and

Table 1
Determination of BPA and 4-CP in food samples by dt-MMIP-SPE in this work: (a) real samples and (b) real samples after spiking with BPA and 4-CP. All experiments were performed in triplicate (n = 3), and RSD (in%) was calculated as [(standard deviation/mean) x 100].

Order	Matrix	Target analytes	Amount spiked (ng mL^{-1})	Intra-day variability			Inter-day variability		
				Found (ng mL^{-1})	Recovery/%	RSD/%	Found (ng mL^{-1})	Recovery/%	RSD/%
(a) Real samples									
1.	Bottled water extract	BPA	–	0.36	–	3.5	0.35	–	3.9
		4-CP	–	0.33	–	3.5	0.32	–	3.4
2.	Fruit juice sample	BPA	–	0.24	–	3.1	0.23	–	4.0
		4-CP	–	0.16	–	2.9	0.15	–	3.3
3.	Honey sample	BPA	–	0.11	–	3.6	0.10	–	4.4
(b) Real samples spiked with BPA and 4-CP									
1.	Milk sample	BPA	1	0.98	98.9	3.1	0.96	96.8	3.7
			5	4.94	98.9	3.8	4.97	99.4	4.1
			10	9.95	99.5	2.8	9.83	98.3	3.4
		4-CP	1	0.97	97.8	3.9	0.97	97.8	4.0
			5	4.96	99.2	3.2	4.93	98.7	3.2
			10	9.83	98.3	3.0	9.81	98.1	3.1
2.	Tomato sauce	BPA	1	0.95	95.9	3.8	0.95	95.6	4.0
			5	4.86	97.2	2.2	4.97	99.4	2.5
			10	9.84	98.4	2.3	9.85	98.5	2.8
		4-CP	1	0.95	95.5	3.3	0.94	94.9	3.3
			5	4.96	99.3	2.5	4.93	98.7	3.4
			10	9.80	98.0	3.2	9.72	97.2	3.7

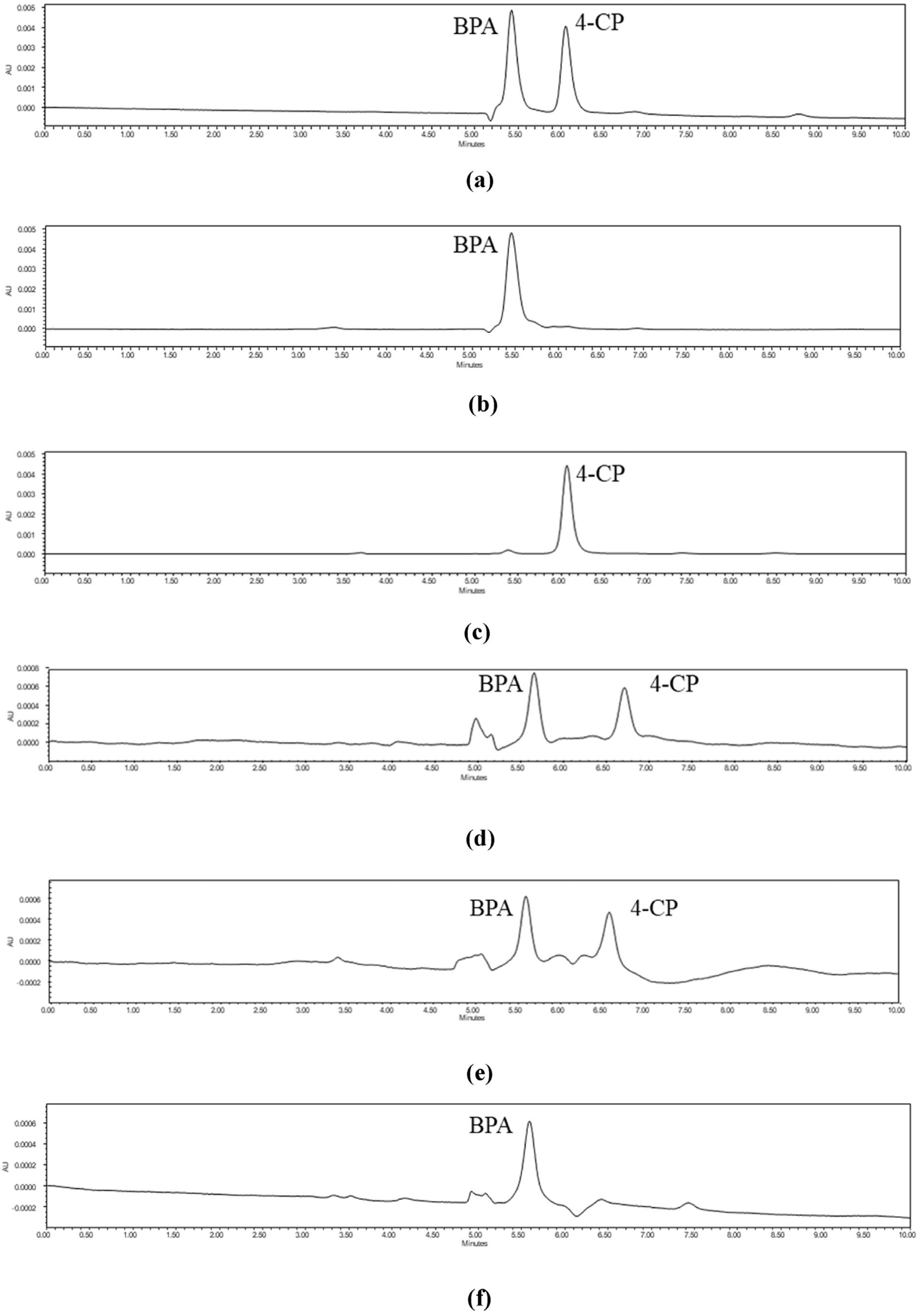

(a)

(b)

(c)

(d)

(e)

(f)

Fig. 4. HPLC chromatogram of (a) standard solution of BPA and 4-CP (1 ng mL^{-1}), (b) standard solution of BPA (1 ng mL^{-1}), (c) standard solution of 4-CP (1 ng mL^{-1}), (d) bottled water extract, (e) fruit juice sample, and (f) honey sample at optimized conditions: mobile phase (MeOH: H_2O; 9:1 (v/v)), flow rate (1 mL min^{-1}), detection wavelength ($\lambda = 278$ nm), injection volume (20 μL), and C-18 column (4.6 × 250 mm).

Table 2
Comparison of BPA and 4-CP determination in food samples among studies.

Order	Type of food samples	Pre-treatment method	Separation and detection method	Analyte	Recovery (%)	Precision RSD (%)	Extraction time (min)	Detection limit (ng mL^{-1})	Reusable cycles	Reference
1.	Bottled water, juice, honey, milk and tomato sauce	dt-MMIP-SPE	HPLC-PDA	BPA, 4-CP	94.9–99.4	<5	5	0.04–0.05[a]	20	This study
2.	Bottled mineral water/bottled milk	SMNM-SBSE	HPLC-UV	BPA	84–102.40	<11	40	0.02–0.38[b]	6–9	Gorji et al. (2019)
3.	Beverage bottle water, juice	Fe_3O_4@MON–NH_2–SPE	HPLC-UV	BPA, 4-CP	80.3–93	<6	40	0.015[b]	4	Du et al. (2020)
4.	Juice	Nano-MIMs/SPE	HPLC-UV	BPA	72.25–89.97	<10	480	5.7[b]	–	Wu et al. (2014)
5.	Milk	MIP-SPE	HPLC-UV	BPA	97.23–99.21	<4	40	3.7	6	Yuan et al. (2016)
6.	Juice	MI-MNPs-d-SPE	HPLC-UV	BPA	93.3–100	5	60	0.3[b]	5	Wu et al. (2017)
7.	Milk	TMIP-SPE	CE-UV/HPLC-UV	BPA	80–85	–	20	–	–	Alenazi et al. (2015)

dt-MMIP SPE: dual-template magnetic molecularly imprinted polymers; TMIP: treated molecularly imprinted polymers; CE-UV: capillary electrophoresis with ultraviolet detection; MIMs/SPE: molecularly imprinted membrane-based solid phase extraction; Fe_3O_4@MON-NH_2: magnetic amino-functionalized micro-porous organic framework composites; SMNM-SBSE: self-magnetic nano-composite monolithic stir bar sorptive extraction; N.D.: not detected.

[a] Detection limit measured in terms of MDL ($MDL = t\,(n-1,\ 1-\alpha = 0.99)\ S$).

[b] Detection limit measured in terms of signal to noise ratio (S/N) = 3.

juice samples when used four times. In comparison, the synthesized dt-MMIP sorbent was tested 25 times for adsorption-desorption tests and exhibited good recovery values (80.0% for BPA and 78.0% for 4-CP) up to the 20th cycle. As such, the method based on dt-MMIP sorbent demonstrated durability and stability and showed efficient recoveries (94.9–99.4%) for BPA and 4-CP in spiked (milk and tomato sauce) samples, with RSD values less than 5%. In addition to this, the dt-MMIP required less extraction time (5 min) than the other reported methods (Table 2), which generally took 20–480 min for extraction. Furthermore, dt-MMIP did not require special instrumentation and showed good clean up of analytes. These results confirm that dt-MMIP-SPE coupled with an HPLC method could be applied for selective and sensitive determination of trace BPA and 4-CP in complicated matrices including foodstuffs.

4. Conclusions

A dt-MMIP material was synthesized for use as an SPE sorbent coupled with HPLC-PDA. The dt-MMIP-based SPE method was applied to simultaneous selective detection of BPA and 4-CP in different food samples using various pre-optimized experimental parameters. The dt-MMIP had high activity and selectivity toward BPA and 4-CP and was highly reusable for 20 cycles. The experimental results indicate that the dt-MMIP-based SPE method can be used as a simple, sensitive, and reliable option for detection of alkylphenol species (e.g., BPA and 4-CP) in foodstuffs with different matrix composition. The method could be developed further to improve sensitivity and selectivity to expand the list of detectable target analytes.

Credit author statement (author role)

Shikha Bhogal; Irshad Mohiuddin; Kuldeep Kaur: Conceptualization; Data curation; Investigation; Formal analysis, Jechan Lee; Richard J. C. Brown: Validation; Visualization; Formal analysis, Ki-Hyun Kim; Ashok Kumar Malik: Investigation; Methodology; Project administration; Resources; Software; Supervision; Validation; Visualization; Writing – review & editing

Declaration of competing interest

The authors declare that they have no known competing financial interests or personal relationships that could have appeared to influence the work reported in this paper.

Acknowledgments

SB, IM, and AKM are thankful to the UGC-SAP and the Chemistry Department, Punjabi University, Patiala, for providing lab and instrument facilities. KK is thankful to Mata Gujri College, Fatehgarh Sahib, Punjab, for providing lab facilities. KHK acknowledges support by the R&D Center for Green Patrol Technologies through the R&D for Global Top Environmental Technologies funded by the Ministry of Environment (MOE), as well as a grant from the National Research Foundation of Korea (NRF) funded by the Ministry of Science, ICT, & Future Planning (Grant No: 2016R1E1A1A01940995).

Appendix A. Supplementary data

Supplementary data to this article can be found online at https://doi.org/10.1016/j.envpol.2021.116613

References

Alenazi, N.A., Manthorpe, J.M., Lai, E.P., 2015 Apr 1. Selective extraction of BPA in milk analysis by capillary electrophoresis using a chemically modified molecularly imprinted polymer. Food Contr. 50, 778–783.

Almeida, S., Raposo, A., Almeida-González, M., Carrascosa, C., 2018. Bisphenol A: food exposure and impact on human health. Compr. Rev. Food Sci. Food Saf. 17, 1503–1517.

Ansari, S., 2017. Application of magnetic molecularly imprinted polymer as a versatile and highly selective tool in food and environmental analysis: recent developments and trends. Trac. Trends Anal. Chem. 90, 89–106.

Arabi, M., Ghaedi, M., Ostovan, A., 2017. Development of a lower toxic approach based on green synthesis of water-compatible molecularly imprinted nanoparticles for the extraction of hydrochlorothiazide from human urine. ACS Sustain. Chem. Eng. 5, 3775–3785.

Berardi, C., Fibbi, D., Coppini, E., Renai, L., Caprini, C., Scordo, C.V.A., Checchini, L., Orlandini, S., Bruzzoniti, M.C., Del Bubba, M., 2019. Removal efficiency and mass balance of polycyclic aromatic hydrocarbons, phthalates, ethoxylated alkylphenols and alkylphenols in a mixed textile-domestic wastewater treatment plant. Sci. Total Environ. 674, 36–48.

Chiha, M., Hamdaoui, O., Baup, S., Gondrexon, N., 2011. Sonolytic degradation of endocrine disrupting chemical 4-cumylphenol in water. Ultrason. Sonochem. 18, 943–950.

Culita, D.C., Simonescu, C.M., Patescu, R.-E., Dragne, M., Stanica, N., Oprea, O., 2016.

o-Vanillin functionalized mesoporous silica–coated magnetite nanoparticles for efficient removal of Pb (II) from water. J. Solid State Chem. 238, 311–320.

Cesen, M., Lambropoulou, D., Laimou-Geraniou, M., Kosjek, T., Blaznik, U.k., Heath, D., Heath, E., 2016. Determination of bisphenols and related compounds in honey and their migration from selected food contact materials. J. Agric. Food Chem. 64, 8866–8875.

de Oliveira, H.L., Pires, B.C., Teixeira, L.S., Dinali, L.A.F., Simões, N.S., de Souza Borges, W., Borges, K.B., 2019. Novel restricted access material combined to molecularly imprinted polymer for selective magnetic solid-phase extraction of estrogens from human urine. Microchem. J. 149, 104043.

Dil, E.A., Ghaedi, M., Asfaram, A., Mehrabi, F., Shokrollahi, A., Matin, A.A., Tayebi, L., 2020. Magnetic dual-template molecularly imprinted polymer based on syringe-to-syringe magnetic solid-phase microextraction for selective enrichment of p-Coumaric acid and ferulic acid from pomegranate, grape, and orange samples. Food Chem. 126902.

Du, Z.-D., Cui, Y.-Y., Yang, C.-X., Yan, X.-P., 2020. Synthesis of magnetic amino-functionalized microporous organic network composites for magnetic solid phase extraction of endocrine disrupting chemicals from water, beverage bottle and juice samples. Talanta 206, 120179.

Gao, R., Hao, Y., Zhao, S., Zhang, L., Cui, X., Liu, D., Tang, Y., Zheng, Y., 2014a. Novel magnetic multi-template molecularly imprinted polymers for specific separation and determination of three endocrine disrupting compounds simultaneously in environmental water samples. RSC Adv. 4, 56798–56808.

Gao, R., Mu, X., Hao, Y., Zhang, L., Zhang, J., Tang, Y., 2014b. Combination of surface imprinting and immobilized template techniques for preparation of core–shell molecularly imprinted polymers based on directly amino-modified Fe 3 O 4 nanoparticles for specific recognition of bovine hemoglobin. J. Mater. Chem. B 2, 1733–1741.

Gorji, S., Bahram, M., Biparva, P., 2019. Optimized stir bar sorptive extraction based on self-magnetic nanocomposite monolithic kit for determining Bisphenol A in bottled mineral water and bottled milk samples. Anal. Bioanal. Chem. Res. 6, 137–156.

Grover, A., Kaur, R., Mohiuddin, I., Malik, A.K., Aulakh, J.S., Tsang, Y.F., Kim, K.-H., 2019. Surfactant-modified Zn/Al-layered double hydroxides for efficient extraction of alkyl phenols from aqueous samples. Environ. Res. 177, 108605.

Han, S., Li, X., Wang, Y., Su, C., 2014. A core–shell Fe 3 O 4 nanoparticle–CdTe quantum dot–molecularly imprinted polymer composite for recognition and separation of 4-nonylphenol. Anal. Methods 6, 2855–2861.

Hu, C., Deng, J., Zhao, Y., Xia, L., Huang, K., Ju, S., Xiao, N., 2014. A novel core–shell magnetic nano-sorbent with surface molecularly imprinted polymer coating for the selective solid phase extraction of dimetridazole. Food Chem. 158, 366–373.

Jafari, M.T., Rezaei, B., Bahrami, H., 2018. Magnetic dual-template molecularly imprinted polymer nanoparticles for the simultaneous determination of acetaminophen and codeine in urine samples by ion mobility spectrometry. Anal. Sci. 34, 297–303.

Kubiak, A., Biesaga, M., 2019. Application of molecularly imprinted polymers for bisphenols extraction from food samples–A review. Crit. Rev. Anal. Chem. 1–11.

Lahcen, A.A., Amine, A., 2019. Recent advances in electrochemical sensors based on molecularly imprinted polymers and nanomaterials. Electroanalysis 31, 188–201.

Liu, H., Chen, W., 2015. Magnetic mesoporous imprinted adsorbent based on Fe 3 O 4-modified sepiolite for organic micropollutant removal from aqueous solution. RSC Adv. 5 (34), 27034–27042.

Liu, J., Wang, W., Xie, Y., Huang, Y., Liu, Y., Liu, X., Zhao, R., Liu, G., Chen, Y., 2011. A novel polychloromethylstyrene coated superparamagnetic surface molecularly imprinted core–shell nanoparticle for bisphenol A. J. Mater. Chem. 21, 9232–9238.

Lu, W., Wang, X., Wu, X., Liu, D., Li, J., Chen, L., Zhang, X., 2017. Multi-template imprinted polymers for simultaneous selective solid-phase extraction of six phenolic compounds in water samples followed by determination using capillary electrophoresis. J. Chromatogr. A 1483, 30–39.

Lu, Y.C., Guo, M.H., Mao, J.H., Xiong, X.H., Liu, Y.J., Li, Y., 2019. Preparation of core-shell magnetic molecularly imprinted polymer nanoparticle for the rapid and selective enrichment of trace diuron from complicated matrices. Ecotoxicol. Environ. Saf. 177, 66–76.

Mahmoudi, M., Simchi, A., Imani, M., Milani, A.S., Stroeve, P., 2008. Optimal design and characterization of superparamagnetic iron oxide nanoparticles coated with polyvinyl alcohol for targeted delivery and imaging. J. Phys. Chem. B 112, 14470–14481.

Mohiuddin, I., Grover, A., Aulakh, J.S., Lee, S.-S., Malik, A.K., Kim, K.-H., 2020. Porous molecularly-imprinted polymer for detecting diclofenac in aqueous pharmaceutical compounds. Chem. Eng. J. 382, 123002.

Muratsugu, S., Shirai, S., Tada, M., 2020. Recent progress in molecularly imprinted approach for catalysis. Tetrahedron Lett. 61, 151603.

O'Neill, D.T., Rochette, E.A., Ramsey, P.J., 2002. Method detection limit determination and application of a convenient headspace analysis method for methyl tert-butyl ether in water. Anal. Chem. 74, 5907–5911.

Peng, Y., Xie, Y., Luo, J., Nie, L., Chen, Y., Chen, L., Du, S., Zhang, Z., 2010. Molecularly imprinted polymer layer-coated silica nanoparticles toward dispersive solid-phase extraction of trace sulfonylurea herbicides from soil and crop samples. Anal. Chim. Acta 674, 190–200.

Sullivan, M.V., Dennison, S.R., Archontis, G., Reddy, S.M., Hayes, J.M., 2019 May 31. Toward rational design of selective molecularly imprinted polymers (MIPs) for proteins: computational and experimental studies of acrylamide based polymers for myoglobin. J. Phys. Chem. B 123 (26), 5432–5443.

Surikumaran, H., Mohamad, S., Muhamad Sarih, N., Raoov, M., 2015. β-Cyclodextrin based molecularly imprinted solid phase extraction for class selective extraction of priority phenols in water samples. Separ. Sci. Technol. 50, 2342–2351.

Wang, B., Huang, B., Jin, W., Wang, Y., Zhao, S., Li, F., Hu, P., Pan, X., 2012. Seasonal distribution, source investigation and vertical profile of phenolic endocrine disrupting compounds in Dianchi Lake, China. J. Environ. Monit. 14, 1274–1281.

Wei, S., Li, J., Liu, Y., Ma, J., 2016. Development of magnetic molecularly imprinted polymers with double templates for the rapid and selective determination of amphenicol antibiotics in water, blood, and egg samples. J. Chromatogr. A 1473, 19–27.

Wu, Y.-t., Zhang, Y.-h., Zhang, M., Liu, F., Wan, Y.-c., Huang, Z., Ye, L., Zhou, Q., Shi, Y., Lu, B., 2014. Selective and simultaneous determination of trace bisphenol A and tebuconazole in vegetable and juice samples by membrane-based molecularly imprinted solid-phase extraction and HPLC. Food Chem. 164, 527–535.

Wu, X., Li, Y., Zhu, X., He, C., Wang, Q., Liu, S., 2017 Jan 1. Dummy molecularly imprinted magnetic nanoparticles for dispersive solid-phase extraction and determination of bisphenol A in water samples and orange juice. Talanta 162, 57–64.

Yang, R., Liu, Y., Yan, X., Liu, S., Zheng, H., 2016. An effective method for the synthesis of yolk–shell magnetic mesoporous carbon-surface molecularly imprinted microspheres. J. Mater. Chem. 4, 9807–9815.

Young, T., Geng, M., Lin, L., Thagard, S.M., 2013. Oxidative degradation of Bisphenol A: a comparison between Fenton reagent, UV, UV/H2O2 and ultrasound. J. Adv. Oxid. Technol. 16, 89–101.

Yuan, Y., Liu, Y., Teng, W., Tan, J., Liang, Y., Tang, Y., 2016 Sep 2. Preparation of core-shell magnetic molecular imprinted polymer with binary monomer for the fast and selective extraction of bisphenol A from milk. J. Chromatogr. A 1462, 2–7.

Zuo, Y., Zhu, Z., 2014. Simultaneous identification and quantification of 4-cumylphenol, 2, 4-bis-(dimethylbenzyl) phenol and bisphenol A in prawn Macrobrachium rosenbergii. Chemosphere 107, 447–453.